



UNIVERSITY OF LEEDS

This is a repository copy of *Synthesis of quinoline liquid crystals by inverse electron demand Diels-Alder cycloaddition*.

White Rose Research Online URL for this paper:

<https://eprints.whiterose.ac.uk/227219/>

Version: Accepted Version

Article:

Fritsch, L., Moura e Silva, S., Baptista, L.A. et al. (2 more authors) (2025) Synthesis of quinoline liquid crystals by inverse electron demand Diels-Alder cycloaddition. Tetrahedron, 183. 134722. ISSN 0040-4020

<https://doi.org/10.1016/j.tet.2025.134722>

This is an author produced version of an article published in Tetrahedron made available under the terms of the Creative Commons Attribution License (CC-BY), which permits unrestricted use, distribution and reproduction in any medium, provided the original work is properly cited.

Reuse

This article is distributed under the terms of the Creative Commons Attribution (CC BY) licence. This licence allows you to distribute, remix, tweak, and build upon the work, even commercially, as long as you credit the authors for the original work. More information and the full terms of the licence here:

<https://creativecommons.org/licenses/>

Takedown

If you consider content in White Rose Research Online to be in breach of UK law, please notify us by emailing eprints@whiterose.ac.uk including the URL of the record and the reason for the withdrawal request.



eprints@whiterose.ac.uk
<https://eprints.whiterose.ac.uk/>

Synthesis of Quinoline Liquid Crystals by Inverse Electron Demand Diels-Alder Cycloaddition.

Luma Fritsch,¹ Sidnei Moura e Silva,² Luis A. Baptista,³ Richard J. Mandle,^{4,5} Aloir A. Merlo^{1*}

¹ Chemistry Institute, Universidade Federal do Rio Grande do Sul (UFRGS), RS, Brazil.

<https://orcid.org/0000-0001-9949-8010> and <https://orcid.org/0000-0002-8071-5297>

² Biotechnology Institute, Universidade de Caxias (UCS), RS, Brazil

<https://orcid.org/0000-0003-1903-6735>

³ Max Planck Institute for Polymer Research, Mainz, Germany.

<https://orcid.org/0000-0002-1419-6070>

⁴ School of Physics and Astronomy, University of Leeds, UK, LS2 9JT.

⁵ School of Chemistry, University of Leeds, UK, LS2 9JT

<https://orcid.org/0000-0001-9816-9661>

*Corresponding author email: aloir.merlo@ufrgs.br

Abstract

Tetrahydroquinolines (THQ) cycloadducts, as well as their oxidation to the corresponding quinolines are reported. THQs were achieved through the Inverse Electron Demand [4+2]-Diels–Alder (IEDDA) cycloaddition. The [4+2]-IEDDA cycloadducts were obtained through a three-component reaction involving aromatic aldehydes, amines and pyrano dienophile, in the presence of TEMPOL (4-hydroxy-2,2,6,6-tetramethylpiperidine-1-oxyl), trifluoroacetic acid and acetonitrile, in low yields < 40%. Theoretical studies were complimentary performed to analyze the chemical reactivity, regio- and stereoselectivity of the IEDDA cycloaddition. The preference for the formation of the THQs cycloadducts was dictated by frontier orbital molecular (FOMs) LUMO of 2-azadieno and HOMO of the dienophile. Oxidation of the THQs with DDQ yielded quinolines in high yields > 90%. The thermal behavior of the THQs and quinolines was studied using DSC and POM techniques. The final quinolines exhibited an amorphous appearance with vitreous, glossy, and brittle characteristics. Through POM studies only one quinoline displayed stable liquid crystal behavior with a glass transition temperature (T_g) and glassy nematic mesophase at room temperature was assigned, without no thermal decomposition detected after cycles of heating and cooling.

Keywords

Aza-Diels-Alder, THQ cycloadducts, Quinolines, Liquid Crystals and DFT calculation.

Highlights

- Aza-Diels-Alder reaction applied to the synthesis of tetrahydroquinolines and the corresponding oxidation step to quinolines;
- Three-component protocol using aldehydes and aromatic amines and polarophiles;
- Nematic liquid-crystalline mesophase;
- Shiny and glassy material;

1. Introduction

The Diels-Alder reaction (DA) is a powerful and widely used synthetic tool for the preparation of cyclic compounds. The DA reaction is widely used in the synthesis of natural products,[1-3] owing to its control over regio- and stereo-chemistry. The DA reaction can utilize a diverse array of dienes and dienophiles, and thus can be used to construct molecules of essentially arbitrary complexity. The DA reaction is a [4+2]-cycloaddition and depending on the electronic nature of the two components involved in the reaction, the terms "Direct Electron Demand Diels-Alder reactions" (DEDDA or simply DA) and "Inverse Electron Demand Diels-Alder reactions" (IEDDA) are employed. As a general rule, the term direct demand DA reaction is used when the dienophile is an alkene substituted by Electron-Withdrawing Groups (EWG), whereas inverse electron demand denotes a dienophile that is an alkene substituted by Electron-Donating Groups - EDG.[4]

When the Diels-Alder reaction is employed for the synthesis of functionalized heterocycles, it bears the prefix "hetero" to denote that one of the components of the reaction contains heteroatoms in its structure (e.g., N and O). A common subclass of hetero-Diels-Alder reactions is represented by aza-DA, which involves either an aza-dienophile or an aza-diene.[5]

The [4+2] cycloaddition involving aza-imines or aza-dienes is a well-established and efficient method for synthesizing quinoline derivatives. Since Povarov's pioneering work,[6, 7] the aza-Diels-Alder (aza-DA) reaction - typically catalyzed by Lewis acids like $\text{BF}_3 \cdot \text{etherate}$ or trifluoroacetic acid - has been widely employed for this purpose. Quinolines and other six-membered nitrogen heterocycles are key motifs in natural products with broad biological activity[8, 9] and also find use in technologies such as fluorescent materials,[10-12] solar cells,[13] batteries, and liquid crystals.[14-16] In this study, we report the synthesis of tetrahydroquinolines (THQs) via an aza-Diels-Alder reaction between imines and EDG-dienophiles, followed by oxidation to quinolines. Previously, quinolines were synthesized through Lewis acid-mediated three-component reactions[12, 17, 18] [19]involving aromatic aldehydes, amines, and alkynes. Considering our previous work with Schiff base liquid crystals, [20, 21] we proposed that their imine moiety could serve as an electron-withdrawing 2-azadiene in IEDDA reactions with EDG-substituted dienophiles.[22]

Our recent studies show that while aromatic imines (Schiff bases) are thermally and photochemically unstable under harsh conditions,[23-25] they still exhibit strong anisotropy, broad mesophase ranges, and striking liquid-crystalline textures.[21, 26] Due to the chemical and photophysical instability of these compounds, which limits their use in liquid crystal

displays,[24] we propose a synthetic approach to overcome these drawbacks and enhance their practical applicability.

In this direction, we expose the possibility of conducting an IEDDA cycloaddition reaction, wherein the electron-withdrawing group 2-azadiene is derived from liquid-crystalline Schiff bases and the EDG-dienophile is appropriately chosen to fulfill the chemical transformation and yield the corresponding [4+2]-cycloadduct tetrahydroquinoline. To address the thermal and photophysical instability of previously studied Schiff bases, [23, 27] we synthesized tetrahydroquinoline cycloadducts and converted them into quinoline derivatives. The resulting compounds were then evaluated for their liquid-crystalline properties, which are discussed in this work.

2. Synthesis

The IEDDA cycloadducts tetrahydroquinolines **5a**, **5b** and **6** were synthesized according to Scheme 1. The cycloadducts were obtained from a three-component approach instead of two-component way. The overall process involves the use of aniline, aldehyde, and dienophile in the presence of a Lewis acid catalyst. The aza-diene is produced in situ, without isolation, and is captured by the dienophile present in the acidic reaction medium. This multicomponent reaction is known as Povarov reaction largely applied in the synthesis of 6-membered *N*-containing heterocycles. Alternatively, in the two-component approaches the imines were synthesized and isolated as solid and solubilized in toluene to react with dienophiles in the presence of a Lewis catalyst. Independently if the protocol to access tetrahydroquinolines is two- or three-component, the final step was the oxidation of tetrahydroquinoline nuclei with 2,3-dichloro-5,6-dicyanobenzoquinone (DDQ) to generate the flat and full-conjugated quinoline ring. Fig. 1 outlines the approach for the synthesis of aza-Diels-Alder cycloadducts and the oxidation step to the final quinolines.

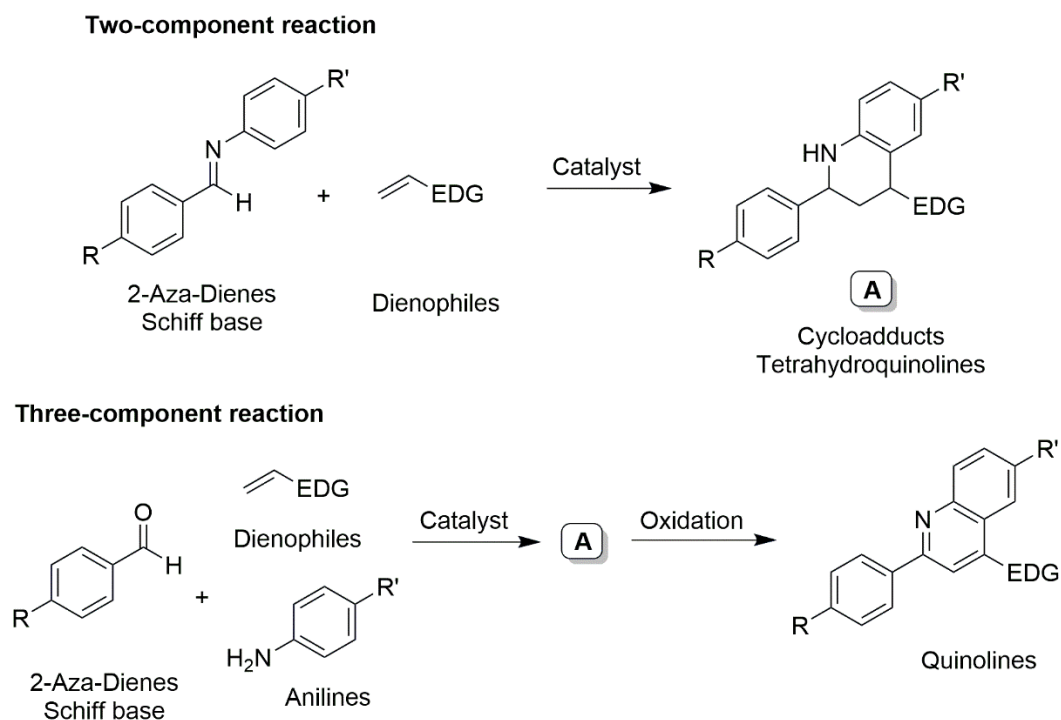


Figure 1. General strategies to the synthesis of cycloadducts **A** and their oxidation step.

The multicomponent Povarov reaction,[28-31] involving three reactive components, is carried out in a catalytic environment mediated by a Brönsted acid such as trifluoroacetic acid or Lewis acid such as BF_3 . The coordination with the in situ formed imine intermediate is the most critical aspect to produce the desired cycloadduct in a reasonable yield.[32, 33]

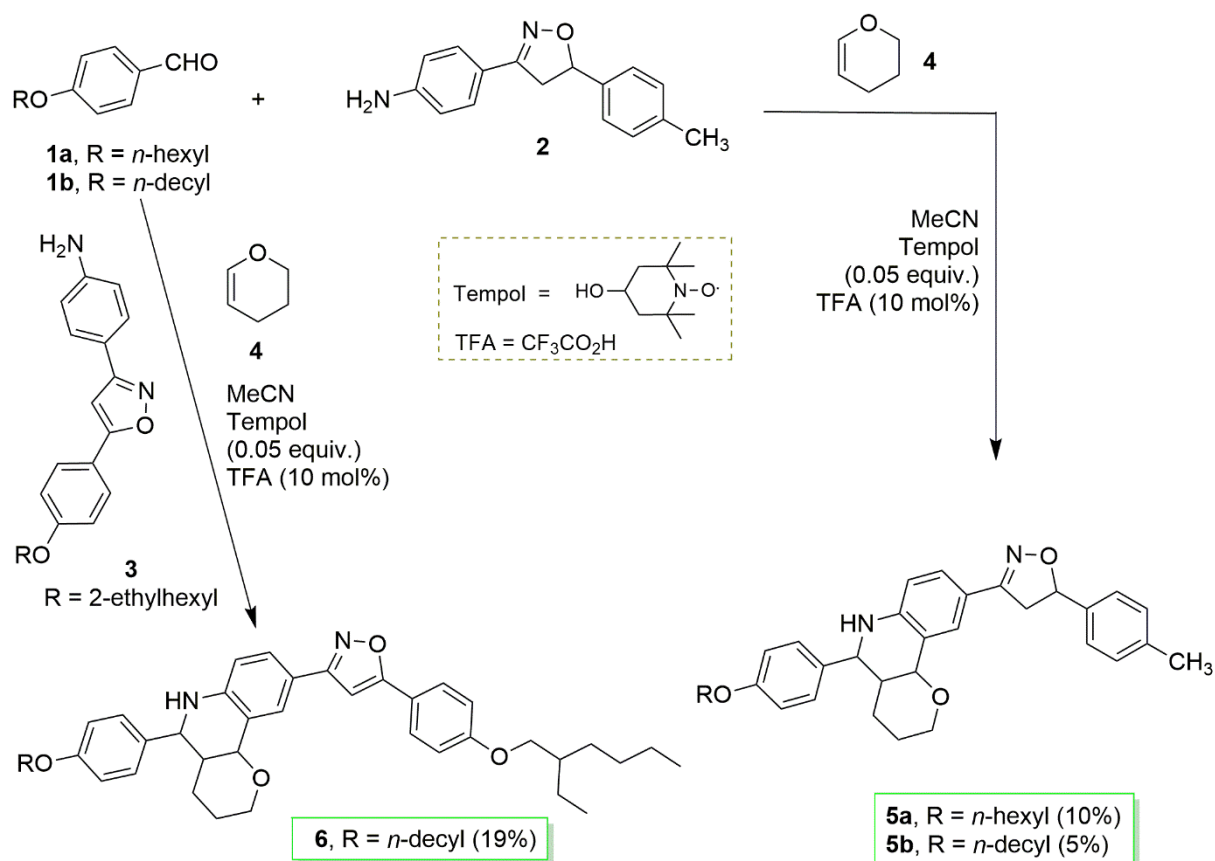
Scheme 1 outlined the synthesis of cycloadduct tetrahydroquinolines **5a**, **5b** and **6** based on three-component process. The first component aldehydes **1a,b** were prepared by alkylation reaction of the 4-hydroxybenzaldehyde, while 5-membered isoxazoline **2** and isoxazole **3** were obtained by 1,3-dipolar cycloaddition and the corresponding oxidation step to yield the isoxazole derivative.[21, 24] Commercial dipolarophile 3,4-dihydro-2H-pyran (DHP) (**4**) was used to complete the synthesis of six-membered tetrahydroquinolines as a pre-mesogenic intermediates, using trifluoroacetic acid.[34] The IEDDA reaction was unproductive with the use of other dienophiles such as vinyl ethyl ether, cyclohexene, and succinic anhydride.

After conducting a comprehensive analysis of the reaction conditions involving different solvents, acid catalysts, temperature, reaction times, and reagents that proved to be unproductive and non-reproducible, we found that the combination yielding the DA aza-cycloadduct in modest to poor yield involved the introduction of an additive into the reaction

along with trifluoroacetic acid (TFA) and acetonitrile (MeCN) as solvent. The catalytic additive TEMPOL (4-hydroxy-2,2,6,6-tetramethylpiperidine-1-oxyl)[35] was used (0.05 equiv.) for synthesis of cycloadducts **5a**, **5b** and **6** in TFA 10%. Using this protocol reaction, THQs bearing the isoxazoline ring were obtained in yields of 10% (**5a**) and 5% (**5b**). For THQ **6** having the isoxazole ring the reaction yield was 19% in the same reaction conditions. Attempts to obtain **6** without the addition of the TEMPOL additive were unsuccessful, resulting either in the recovery of some of the reagents used or the decomposition of the reagents employed. The function of this additive is not clear from the mechanism point of view. Leardini and coworkers reported the quinolines LC by cyclization steps mediated by radical species,[36] while Fritsch reported a photochemical studies related to the decomposition of azadienes in solution with participation of diradical species at excited state.[23] An increase from 10% to 80% of trifluoroacetic acid showed a higher yield for obtaining **6**, from 19% to 41% yield.

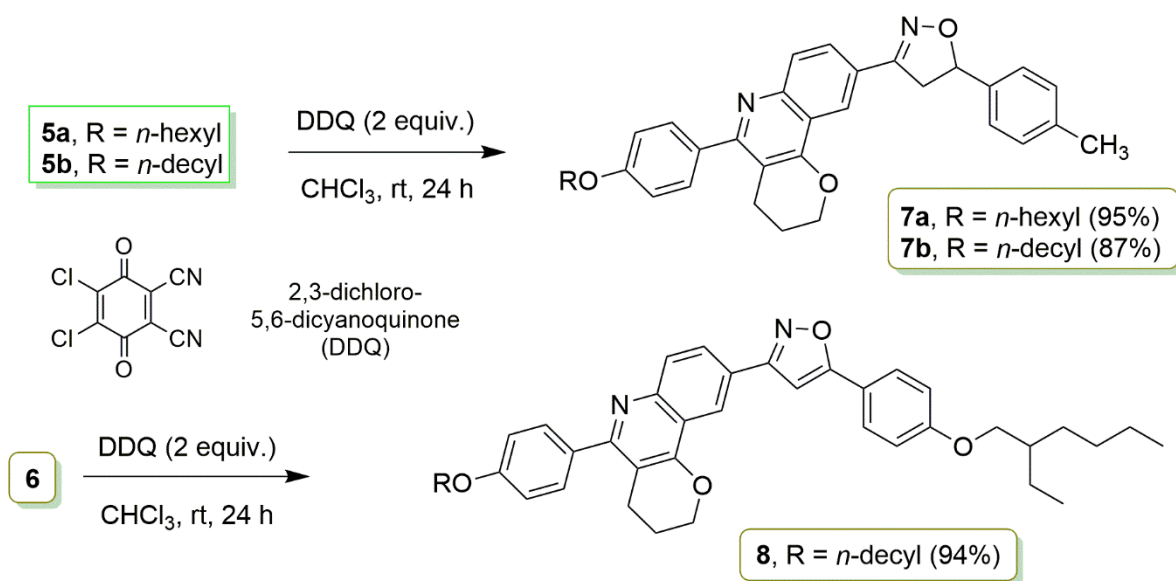
Attempts to performed IEDDA cycloaddition reaction using vinyl ethyl ether as a second dienophile using acid catalyst beyond TFA such as Yb(OTf)₃, [12], [17] iodine, [37] [38] and others [39], [40] have failed to isolate the THQ cycloadducts.

By analysis using ¹H NMR spectrum data of the unpurified material isolated after extraction revealed the decomposition of the vinyl ethyl ether and traces of aldehyde and Schiff base. The repeated failures in synthesis attempts using alternative dienophiles may be attributed to the instability of the imines formed *in situ*, particularly when vinyl ethyl ether is employed. As previously noted, the successful DA reactions were those in which the cycloadduct precipitated from the reaction medium during the course of the reaction, despite the low yields of THQs. Consequently, the formation of a less soluble cycloadduct represents a competitive mechanism with the decomposition of the pre-formed imine in solution.



Scheme 1. Aza-Diels-Alder reaction for the synthesis of tetrahydroquinolines (THQs)

The final stage of forming quinolines **7a**, **7b**, and **8** from tetrahydroquinolines **5a**, **5b** and **6** was accomplished using 2,3-dichloro-5,6-dicyano-1,4-benzoquinone (DDQ) as the oxidizing agent, as depicted in Scheme 2. The oxidation reaction was conducted in chloroform under stirring at rt for 24h. The reaction was quenched by the addition of a saturated sodium bicarbonate solution, followed by the separation of the organic phase and extraction with chloroform. The resulting solids were recrystallized in ethanol, yielding **7a** (95%), **7b** (87%), and **8** (94%).



Scheme 2. Oxidation process mediated by 2,3-dichloro-5,6-dicyanoquinone (DDQ).

3. NMR Data for [4+2]-Diels-Alder THQ Cycloadducts.

The assignment of relative stereochemistry to the THQ cycloadduct obtained in the aza-Diels-Alder reaction was performed through analysis of ^1H and ^{13}C NMR spectra, as well as two-dimensional COSY (CORrelated SpectroscopY) and HSQC (Heteronuclear Single Quantum Correlation) spectra.

In the Diels-Alder reaction involving an aza-2-diene and a *cis*-alkene dienophile, two diastereoisomers can form based on the *endo* or *exo* approach of the dienophile. Both approaches yield *cis*-fused tetrahydroquinolines (THQs) due to the *cis* configuration of the dienophile. However, the stereochemistry of the hydrogen atom on aza-2-diene in the THQs can be *cis* or *trans* depending on its spatial relationship to nearby hydrogens on the six-membered tetrahydropyridine (THP) ring. Figure 2 shows the general structure of *cis*-fused THQs highlighting hydrogen atoms Ha, Hb, and Hc in chair conformation. The relative stereochemistry of the Diels-Alder adducts was determined by analyzing the ^1H - ^1H coupling constant ($J_{a,b}$) between Ha and Hb and comparing the values to literature. *Endo* adducts exhibit smaller $J_{a,b}$ values (5.5–5.7 Hz), consistent with a gauche conformation where the pyran ring and aryl group are on the same side. In contrast, *exo* adducts show larger $J_{a,b}$ values (8.1–11.1 Hz), indicating an *anti* orientation of H_a/H_b with the pyran and aryl groups on opposite sides of the quinoline ring.[39, 41]

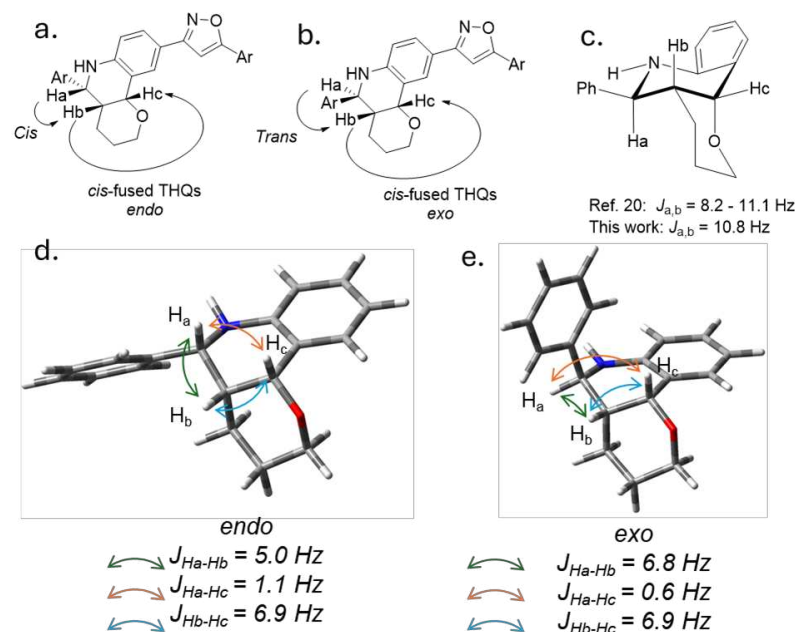


Figure 2. Relative orientation of aryl group and 6-membered THP ring in (a) *endo*- and (b) *exo*-adducts *cis*-fused THQs. <<what about (c)>>; DFT optimized structures (B3LYP-GD3BJ/cc-pVTZ level) for the *endo* (d) and *exo* (e) configurations of a simple phenyl substituted THQ cycloadduct with calculated NMR spin-spin coupling constants (J) given for the indicated atoms.

As a final demonstration of the stereoselectivity of the aza-DA reaction we obtained optimized geometries of the *endo-cis* and *exo-cis* forms at the B3LYP-GD3BJ/cc-pVTZ level of DFT in Gaussian G16 rev C02 [with Int = Ultrafine, Opt = VeryTight, and solvation via scrf = (solvent = chloroform, pcm)]. Next, we computed the NMR shifts using the Gauge-Independent Atomic Orbital (GIAO) method along with spin-spin couplings for all atoms, at the same level of theory and solvation. Thus, we can then compare the experimental NMR coupling constants with those obtained from DFT (Fig 2d, 2e) which match the experimental trend albeit with some deviation in absolute terms.

Thus, through ^1H and ^{13}C [^1H NMR] spectra, as well as two-dimensional COSY and HSQC spectra the cycloadducts **5a**, **5b** and **6** were isolated and characterized. The relevant spectroscopic data is related to the coupling constant (J) determined for *cis*-fused THQs in this aza-DA reaction. In the current work, the coupling constant values found for the isolated cycloadducts indicated the formation of *exo-cis*-fused THQ cycloadducts, which showed a coupling constant $J_{a,b}$ of 10.8 Hz for the hydrogen nuclei H_a and H_b highlighted in Figure 2, and this is consistent with spectroscopic data from other *exo-cis*-fused THQs published in the literature.[41]

4. Theoretical calculations

The spectroscopic properties of DHQs were explained using energy minimization and theoretical calculations. Quantum calculations, conducted with ORCA 5.0.4[42] and the DFT method, accounted for solvent effects (acetonitrile) using the CPCM model.[43] HOMO and LUMO contours and relative energies were calculated for THQ **5a** precursor. Thus, DFT data were computed for the HOMO and LUMO frontier orbitals of the imine (R = *n*-hexyl), which represent the reactive aza-2-diene formed *in situ* and the dienophile DHP (**4**) used in the three-component aza-DA reaction. The optimal reactant approach in the Diels-Alder reaction is determined by the combination with the smallest energy gap between the frontier orbitals, based on calculated relative energies.

According to Figure 3, the smallest energy gap is observed in the interaction between the LUMO of the 2-aza-diene and HOMO of dienophile **4** during the aza-DA reaction course. The energies of the frontier molecular orbitals (FMO) of the preformed 2-aza-diene and **4** are shown in Fig. 3b. The values of the energy of the highest occupied molecular orbital (HOMO) of both molecules are -5.77 eV and -6.02 eV, respectively. However, the largest difference of the energy values of the lowest unoccupied molecular orbital (LUMO) between pre-formed 2-aza-diene (-1.92 eV) and **4** (+0.71 eV) defines which is the best combination between OMFs in this chemical approach. Thus, the cycloadduct should be formed between the HOMO of the **4** and LUMO of the pre-formed aza-2-diene as indicates by the dash line in Fig. 3b in this IEDDA cycloaddition. In a subsequent step, the approach of dienophile **4** was predicted from orbital symmetry, with C3's higher nucleophilicity (HOMO) targeting the more electrophilic C4 or C6 of the aza-diene (LUMO).

This consideration is based on the coefficients of the 3p orbitals, that compose the FMO of carbon atoms C1 and C4 in the 2-azadiene relative to nitrogen atom N3 and carbon atom C6 in the 1-azadiene, respectively. The LUMO coefficients values on C4 (+ 0.167) and C6 (+ 0.189) carbon atoms in two potential reactive aza-diene are very close in size. However, for terminal C1 carbon atom at the LUMO display very low value (+ 0.076) in electrophilicity ensures the formation of the predictable regioisomer. Inversely, the aza-diene's HOMO shows highest electron density at C1, driven by alkoxy-induced delocalization, favoring formation of the 2-azadiene regioisomer rather than the 1-azadiene, which is supported by Fukui electrophilic index analysis.

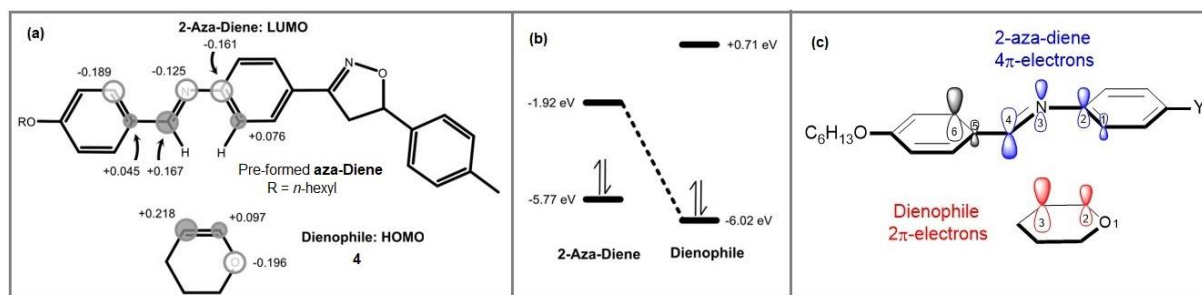


Figure 3. (a) Lowest unoccupied molecular orbital (LUMO) for aza-2-diene and highest occupied molecular orbital (HOMO) for dienophile THP (**4**); (b) Energy values and HOMO–LUMO energy gaps; (c) Interaction between aza-2-diene (LUMO) and dienophile **4** (HOMO) is driven by HOMO and LUMO coefficients (contour orbitals) leading the correct formation of *exo-cis*-fused THQs regioisomer.

Fig. 4 describes the energetic profile for aza-DA reaction constructed by extracting the free energy differences (ΔG), which helps to understand better which reaction site is preferred during the approach of reactants in the transition state, between two possibilities of the interaction for the DHP **4** and preformed aza-diene. The first possibility occurs through the electronic interaction of the C1 and C2 carbon atoms of DHP with C1 and C4 carbon atoms of the 2-aza-diene, respectively. This combination yields two possible cycloadduct named as *endo*- and *exo*-adducts *cis*-fused THQs (Fig 2 and 3a). Theoretical calculations showed that cycloadduct formation via the aza-1-diene is energetically less favorable than with the aza-2-diene, involving bond between DHP's C1–C2 and the aza-1-diene's N and C6 atoms. (see Fig. 3c).

As shown in Fig. 4, the attack of the DHP in the aza-2-diene is energetically favored, since the products of their reaction require at least less 5.0 kcal/mol to be formed than the products in the aza-2-diene. Finally, through energetic profile outlined in Fig 4 it is possible to see that *exo*-adducts *cis*-fused THQs is preferable over the *endo*-adduct *cis*-fused THQs by 0.60 kcal/mol at the transition state and this difference raised to 1.56 kcal/mol in favor of *exo*-adducts *cis*-fused THQs.

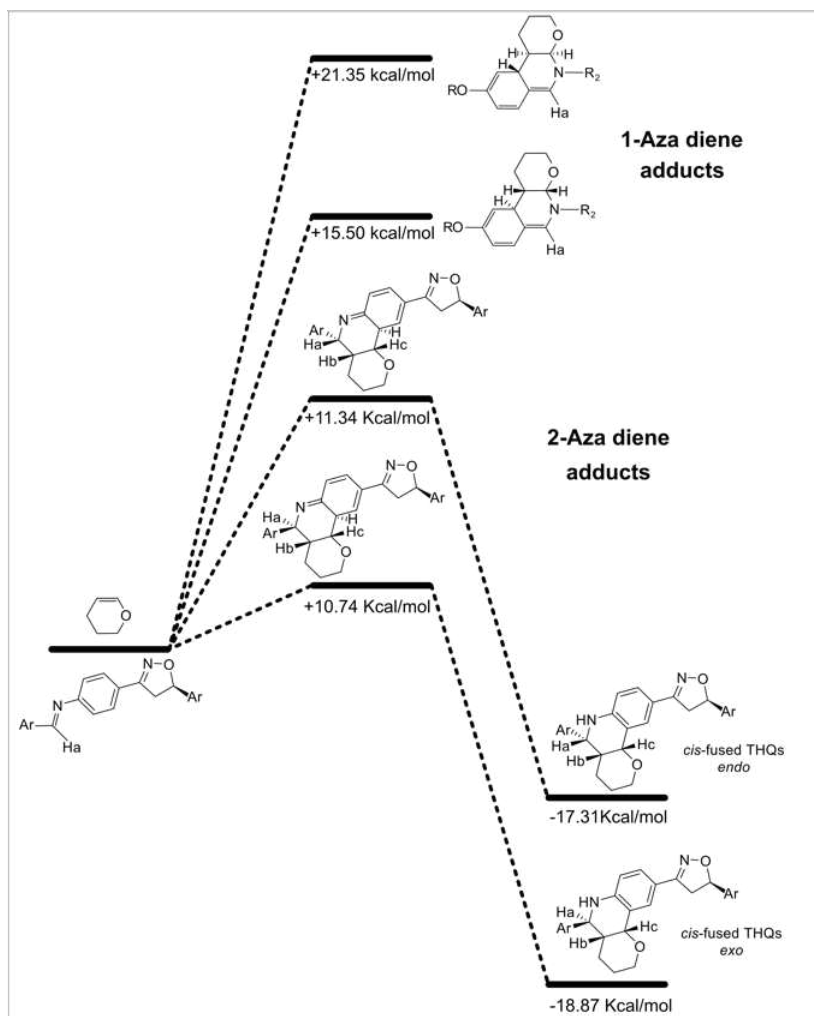


Figure 4. A free-energy profile along a reaction coordinate for the aza-DA reaction in the regime of the acetonitrile solvent. The reaction involves the formation of the active complex (ES) from the dienophile **4** and 1- and 2-aza-diene.

5. Mesomorphic Properties of Quinolines.

The thermal data for THQs and quinolines are tabulated in Table 1, and pictures for nematic mesophase (N) are shown in Fig. 5. The transition temperatures and enthalpy value of the phase transitions were determined by differential scanning calorimetry (DSC) during the second heating cycle for quinolines **7a-b** and **8** with the scan rate at $10\text{ }^{\circ}\text{C}\cdot\text{min}^{-1}$ (Table 1). The melting points for THQs and nematic texture were analyzed by polarized-light optical microscopy (POM).

The THQs **5a-b** and **6** synthesized in this work are amorphous pale white solid with high melting point (mp, Table 1) recorded by POM, and none of them displayed mesomorphic behavior when view between crossed polarizers. For quinolines **7a-b** and **8** obtained by oxidation of the corresponding THQs, yellowish to pale brown solids with like-plastic

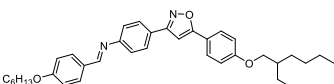
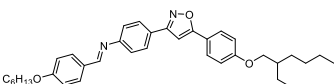
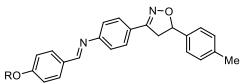
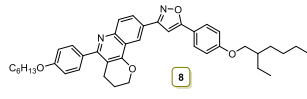
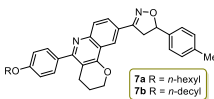
appearance were isolated. From the DSC studies, it was observed that, starting from the second heating cycle, all the quinolines synthesized materials behave as amorphous solids, exhibiting a glass transition temperature (T_g) characteristic of vitreous amorphous materials. For compound **8**, despite no mesophase formation, a glass transition temperature (T_g) at 103°C and the melting temperature (T_m) at 122°C were recorded (Table 1). For **7a** and **8** no mesophase was observed during the heating and cooling cycles.

Quinolines **7a-b** containing 5-membered isoxazoline embedded into their molecular architecture, while quinoline **8** containing the 5-membered isoxazole ring incorporated in its molecular framework. Moreover, **7a-b** presents a very short terminal chain (methyl group) and **8a** display a branch and longer alkyl group represented by 2-ethylhexyl chain (EH group). Liquid-crystalline behavior was detected by POM through the birefringence characteristic exhibited by **7b**. The observed schlieren texture with sand-like grains appearance suggests a lower order mesophase and it was assigned as nematic texture as seen in Fig. 5 (A) and magnification (50x) of nematic texture in Fig 5 (below) for **7b**.

The thermal behavior for THQs and quinolines tabulated in Table 1 and Fig. 5 was altered by the incorporation of second 6-membered heterocycle (pyran ring) into the framework of final the final compounds THQs and quinolines. The presence of pyran ring did not favor the maintenance of mesophases as observed for original 2-azadienes previously reported by our group (footnote in Table 1).[23, 24] The 2-azadienes have showed large mesophase range, such as N, SmA and SmC mesophases. However, the aza-dienos produced in situ are instable and thermal decomposition upon heating was detected when 2-azadienes were exposed upon heating and cooling cycles.

The absence of crystallinity from the second heating cycle can be analyzed through the structure of the final compounds. The central ring, which includes the quinoline ring, is elongated and expanded by the presence of the pyran heterocyclic ring. This portion of the molecule is responsible for the structural rigidity of the synthesized quinolines. The 2 and 6 positions of the quinoline ring contain aromatic substituents, which, in turn, feature flexible chains. The degree of crystallinity is affected by the conformational disorder of the alkyl chains and the rotational disorder of the aryl groups at positions 2 and 6. An increase in the branching of the alkyl group in **7b** promotes the orientational order of the molecules, thereby favoring the emergence of the nematic mesophase. In contrast, the branching in **8** and the shorter alkyl group in **7a** hinder the orientational order and inhibit the formation of the nematic mesophase.

Table 1. Thermal data for THQs and Quinolines recorded by POM and DSC analysis.^a

THQs	Transition temperatures (°C)	Quinolines	Transition temperatures (°C)
5a	mp 190 °C	7a	Tg 34.0 Iso
5b	mp 156 °C	7b	Glass N 38.0 (0,05) Iso
6	mp 155°C	8	Tg 103.0 Tm 122 Iso
<div><div>2-Azadienes</div><div></div><div>Ref. 21/23 R = <i>n</i>-hexyl Cr 143 SmA (135) 144 N 159 I R = <i>n</i>-decyl Cr 138 N 155 I</div><div>Ref. 21 Cr 96 Smc 139 N 173 I</div></div> <div><div>Quinolines in this work</div><div></div><div>7a R = <i>n</i>-hexyl 7b R = <i>n</i>-decyl</div></div>			

^a Tm – melting temperature; Tg – glass transition; N – nematic mesophase; Iso - isotropic state.

The present study revealed that THQs are not liquid crystalline and for quinoline derivatives, only **7b** displayed nematic mesophase (N). We successfully reached our first objective to prepare stable cycloadducts upon heating and cooling cycles without no decomposition as noted by DSC traces. However, final compounds THQs **5a-b** and **6** and quinolines **7a** and **8** lost their mesomorphism except quinoline **7b**. We tentatively assigned the observed thermal behavior to the presence of the pyran ring at the middle of anisotropic core, which destabilizes the mesophase formation by disrupting the balance of anisotropic interactions and packing in the condensed state. Packing consideration is the most likely reason to the disappearance of mesomorphism and the amorphous behavior for all compounds, including the flat quinoline ring against non-planar tetrahydroquinoline. Specifically, the final compound containing branched 2-ethylhexyl chain present a clear polymeric behavior with high Tg temperature and absence of mesophase texture traces.

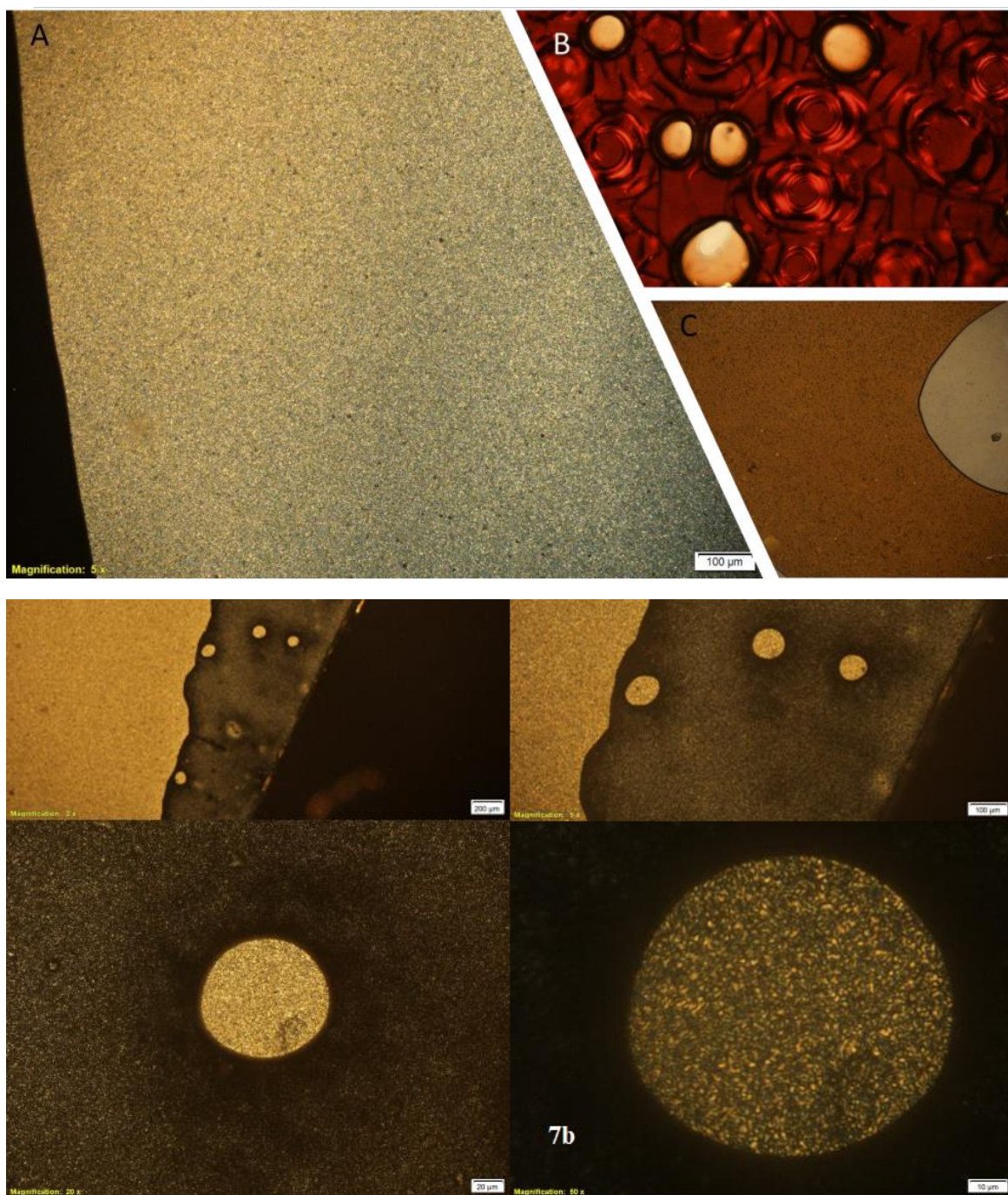


Figure 5. Texture observed by MOLP for quinolines **7b** (A) with crossed polarizers and for **7a** (C); and **8** (B) with uncrossed polarizers (above) and magnification of nematic texture in **7b** (below). Pictures of nematic mesophase in **7b** were taken from the left to right with focus on the yellowish middle circle - magnification of 50x reveals the schlieren texture. The sandy texture with schlieren elements visible only under 50x magnification.

6. Conclusions.

The THQ cycloadducts **5a–b** and **6** were synthesized and oxidized to quinolines **7a–b** and **8** via the Inverse Electron Demand Diels–Alder (IEDDA) reaction.

The [4+2] IEDDA cycloaddition in its three-component version involved aromatic aldehydes **1**, amines **2** and **3**, and the dienophile pyrano **4**, in the presence of TEMPO and trifluoroacetic acid, with yields of less than 40%. The IEDDA reaction was unproductive with the use of other dienophiles such as vinyl ethyl ether, cyclohexene, and succinic anhydride. One of the primary challenges in successfully completing the synthesis was the low solubility of the reagents, particularly amines **2** and **3**. The IEDDA cycloadducts obtained were characterized through ^1H and ^{13}C NMR spectroscopy and thermal analysis. Theoretical studies were performed to analyze the chemical reactivity, regio- and stereoselectivity of FOMs during the IEDDA cycloaddition. The preference for formation of 2-azadiene as described by the THQs cycloadducts **5a–b** and **6** was driven by the energy and reactivity frontier orbital molecular LUMO of 2-azadiene and HOMO of dienophile **4**. A free-energy profile for the aza-DA reaction in acetonitrile determined by DFT demonstrated that the feasibility of the cycloadduct formation reaction arises from the approach of **4** with the 2-aza-diene via the *exo* mode rather than the *endo* mode. Oxidation of the THQs with DDQ yielded quinolines **7a–b** and **8** in high yields. The thermal properties of the THQs and quinolines were analyzed by DSC and POM. The quinolines appeared amorphous, with a glossy, brittle texture. Only quinoline **7b** showed stable liquid crystal behavior, exhibiting a nematic mesophase and a T_g of 38 °C. Despite unsuccessful attempts to synthesize other aza-cycloadducts, the in-situ generation of azadienes from aldehydes and amines with pyrano **4** effectively yielded THQs and their oxidized quinolines. The quinolines showed stable thermal properties, with **7b** exhibiting a nematic glassy mesophase.

7. Experimental

7.1 General Procedure

The solvents for chemical synthesis were purchased from commercial suppliers and were purified according to common procedures. Other chemicals and reagents were commercially available and used as received. Extracts were dried with anhydrous Na_2SO_4 and filtered before removal of the solvent by evaporation. Characterization proton and carbon nuclear magnetic resonance spectra (^1H NMR and ^{13}C NMR) were obtained with CDCl_3 as a solvent on a Varian 400 MHz spectrometer. Chemical shifts are given in parts per million (δ) and are relative to the signal of tetramethylsilane ($\delta = 0$ ppm for ^1H) as internal reference for

solutions in CDCl₃. The NMR spectroscopic data are reported as follows: CDCl₃ (δ = 7.26 ppm for ¹H or δ = 77.1 ppm for ¹³C) and DMSO-d₆ (δ = 2.50 ppm or δ = 49.8 ppm for ¹³C). Multiplicities are reported according to the following abbreviations: s = singlet, d = doublet, t = triplet, q = quartet, m = multiplet, br. = broad. Coupling constants (J) are given in Hz. For the analysis of High-Resolution Mass Spectrometry (HRMS), the compound was dissolved individually in a solution of 1:1 (v/v) chromatographic grade acetonitrile (Tedia®, USA) and ultra-pure water (grade MilliQ®) with addition of 0.1% ammonium formate (negative mode). The solution was infused directly individually into the APCI source by means of a syringe pump (Harvard Apparatus) at a flow rate of 180 $\mu\text{L}\cdot\text{min}^{-1}$. The APCI(+)-MS and tandem APCI(+)-MS/MS were acquired using a hybrid high-resolution and high accuracy (5 $\mu\text{L}\cdot\text{L}^{-1}$) microTof (Q-TOF) mass spectrometer (Bruker® Scientific) under the following conditions: capillary and cone voltages were set to + 3500 V and +40 V, respectively, with a de-solvation temperature of 100°C. For APCI(+)-MS/MS, the energy for the collision induced dissociations (CID) was evaluated in accordance with each compound. For data acquisition and processing in QTOF-control data analysis software (Bruker® Scientific) was used. The data were collected in the m/z range of 70–2000 at the speed of two scans per second, providing the resolution of 50.000 (FWHM) at m/z 200. No important ions were observed below m/z 50 or above m/z 700, therefore APCI(+)-MS data is shown in the m/z 50–900 range. The melting points, phase transition temperatures and mesomorphic textures were taken using an Olympus BX43 microscope equipped with a Mettler Toledo FP82HT Hot Stage with an FP90 Central Processor at a heating/cooling rate of 10 °C.min⁻¹.

7.2 Experimental Procedure. Diels-Alder Cycloaddition reaction.

7.2.1 Representative experimental procedure for synthesis of THQs 5a,b and 6.

In a round-bottom flask, aniline[21] (1 mmol, 1 equiv.), aldehyde (1.1 mmol, 1.1 equiv.), dihydropyran (1.1 mmol, 1.1 equiv.), TEMPOL (0.05 mmol, 0.05 equiv.), and dry acetonitrile (5 mL) were added. The mixture was stirred until homogeneous. Trifluoroacetic acid (0.8 mmol, 0.8 equiv.) was then added dropwise. The reaction was left to stir for 18 h, during which the desired product precipitated. The solid was removed by simple filtration and washed several times with acetonitrile to remove any contaminating material. The obtained solid was then dried under vacuum and studied with further purification.

7.2.2 5-(4-(*n*-Hexyloxy)phenyl)-9-(5-(*p*-tolyl)-4,5-dihydroisoxazol-3-yl) 3,4,4a,5,6,10b-hexahydro-2*H*-pyrano[3,2-*c*]quinoline (**5a**). White solid; yield: 10%; m.p. 190 °C; NMR ¹H (400 MHz, CDCl₃) δ = 7.55 – 7.50 (m, 1H), 7.48 – 7.44 (m, 1H), 7.33 – 7.26 (m, 4H), 7.19 –

7.14 (m, 2H), 6.92 – 6.88 (m, 2H), 6.54 – 6.49 (m, 1H), 5.62 (dd, $J = 10.6, 8.2$ Hz, 1H), 4.68 (d, $J = 10.8$ Hz, 1H), 4.37 (d, $J = 2.6$ Hz, 1H), 4.13 – 4.05 (m, 1H), 3.96 (t, $J = 6.5$ Hz, 2H), 3.76 – 3.59 (m, 2H), 3.31 (dd, $J = 16.4, 8.1$ Hz, 1H), 2.34 (s, 3H), 2.07 – 2.00 (m, 1H), 1.83 – 1.74 (m, 3H), 1.71 – 1.60 (m, 2H), 1.54 – 1.43 (m, 3H), 1.38 – 1.32 (m, 4H), 0.94 – 0.87 (m, 3H). ^{13}C NMR (100 MHz, CDCl_3) δ 159.0; 156.1; 146.4; 138.3; 137.8; 133.4; 130.0; 129.3; 128.7; 128.1; 125.9; 120.1; 118.2; 114.8; 114.2; 81.9; 74.4; 68.7; 68.1; 54.1; 43.4; 38.7; 31.6; 29.5; 25.7; 23.9; 22.6; 21.9; 21.26; 14.1. ESI HRMS m/z calcd for $\text{C}_{34}\text{H}_{41}\text{N}_2\text{O}_3$ $[\text{M} + \text{H}]^+$ 525.3117; found $[\text{M} + \text{H}]^+$ 525.3100.

7.2.3 5-(4-(*n*-Decyloxy)phenyl)-9-(5-(*p*-tolyl)-4,5-dihydroisoxazol-3-yl) 3,4,4a,5,6,10b-hexahydro-2*H*-pyrano[3,2-*c*]quinoline (**5b**). White solid; yield: 5%; m.p. 156 °C; ^1H NMR (CDCl_3 , 400 MHz): δ 7.56 (dd, 1H, $J = 8.5$ Hz, 1.9 Hz); 7.48 (d, 1H, $J = 1.8$ Hz); 7.31 (m, 4H); 7.19 (d, 2H, $J = 8.0$ Hz); 6.93 (d, 2H, $J = 8.5$ Hz); 6.54 (d, 1H, $J = 8.5$ Hz); 5.65 (dd, 1H, $J = 10.6$ Hz, $J = 8.2$ Hz); 4.71 (d, 1H, $J = 10.8$ Hz); 4.40 (d, 1H, $J = 2.6$ Hz); 4.31 (s, 1H); 4.10 (m, 1H); 3.99 (t, 2H, $J = 6.6$ Hz); 3.72 (m, 2H); 3.35 (dd, 1H, $J = 16.5$ Hz, $J = 8.1$ Hz); 2.37 (s, 3H); 2.06 (m, 1H); 1.82 (m, 3 H); 1.68 (m, 1H); 1.48 (m, 4H); 1.34 (m, 12H); 0.91 (t, 3H, $J = 6.8$ Hz). ^{13}C NMR (100 MHz, CDCl_3) δ 159.0; 156.1; 146.4; 138.3; 137.8; 133.4; 130.0; 129.3; 128.7; 128.1; 125.9; 120.1; 118.2; 114.7; 114.2; 81.9; 74.4; 68.7; 68.1; 54.1; 43.4; 38.7; 31.9; 29.6; 29.6; 29.4; 29.3; 29.3; 26.1; 23.9; 22.7; 21.9; 21.2; 14.2. ESI HRMS m/z calcd for $\text{C}_{38}\text{H}_{49}\text{N}_2\text{O}_3$ $[\text{M} + \text{H}]^+$ 581.3743; found $[\text{M} + \text{H}]^+$ 581.3729.

7.2.4 9-(5-(4-((2-Ethylhexyl)oxy)phenyl)isoxazol-3-yl)-5-(4-(*n*-hexyloxy)-phenyl)-3,4,4a,5,6,10b-hexahydro-2*H*-pyrano[3,2-*c*]quinoline (**6**). White solid; yield 41%; m.p. 155 °C; ^1H NMR (CDCl_3 , 400 MHz): δ 7.76 (d, 2H, $J = 8.8$ Hz); 7.73 (d, 1H, $J = 1.9$ Hz); 7.66 (dd, 1H, $J = 8.4$ Hz, 2.0 Hz); 7.34 (d, 2H, $J = 8.6$ Hz); 7.00 (d, 2H, $J = 8.9$ Hz); 6.93 (d, 2H, $J = 8.7$ Hz); 6.67 (s, 1H); 6.61 (d, 1H, $J = 8.4$ Hz); 4.74 (d, 1H, $J = 10.8$ Hz); 4.48 (d, 1H, $J = 2.6$ Hz); 4.30 (s, 1H); 4.15 (m, 1H); 3.99 (t, 2H, $J = 6.6$ Hz); 3.92 (d, 2H, $J = 6.5$ Hz); 3.77 (td, 1H, $J = 11.4$ Hz, 2.4 Hz); 2.11 (m, 1H); 1.80 (m, 5H); 1.48 (m, 8H); 1.37 (m, 8H); 0.96 (m, 9H). ^{13}C NMR (100 MHz, CDCl_3) δ 169.7; 162.8; 160.6; 158.9; 146.2; 133.6; 129.7; 128.7; 127.9; 127.3; 120.5; 118.0; 114.8; 114.7; 114.3; 95.7; 74.5; 70.6; 68.7; 68.1; 54.2; 39.3; 38.8; 34.7; 31.6; 30.5; 29.3; 29.1; 25.7; 24.0; 23.8; 23.1; 22.6; 21.9; 14.1; 14.1; 11.1. ESI HRMS m/z calcd for $\text{C}_{41}\text{H}_{53}\text{N}_2\text{O}_4$ $[\text{M} + \text{H}]^+$ 637.4005; found $[\text{M} + \text{H}]^+$ 637.4013.

7.3. Oxidation procedure

7.3.1 Representative experimental procedure for synthesis of quinolines **7a**, **7b** and **8**.

To a solution containing tetrahydroquinoline **5a-b** and **6** (1 mmol, 1 equiv.) in chloroform (15 mL), DDQ (2 mmol, 2 equiv.) was added, and the mixture was stirred for 24 h at rt in an open vessel. Upon completion of the reaction, a saturated solution of NaHCO₃ (10 mL) was added, and the resulting mixture was extracted with chloroform (3 × 10 mL). The organic phase was dried over magnesium sulfate, filtered, and concentrated using a rotary evaporator. The solvent was completely removed under vacuum for 4 h. The solid was washed with hot ethanol (3 × 30 mL) to remove residual material with no need further purification.

7.3.2 5-(4-(*n*-Hexyloxy)phenyl)-9-(5-(*p*-tolyl)-4,5-dihydroisoxazol-3-yl)-3,4-dihydro-2H-pyrano[3,2-*c*]quinoline (**7a**). Pale brown solid; yield: 95%; Tg 34°C; ¹H NMR (CDCl₃, 400 MHz) δ = 8.21 – 8.16 (m, 2H); 8.04 (d, *J* = 8.7 Hz, 1H); 7.53 (d, *J* = 8.7 Hz, 2H); 7.31 (d, *J* = 8.1 Hz, 2H); 7.19 (d, *J* = 7.9 Hz, 2H); 6.98 (d, *J* = 8.7 Hz, 2H); 5.76 (dd, *J* = 10.9, 8.4 Hz, 1H); 4.55 – 4.40 (m, 2H); 4.00 (t, *J* = 6.6 Hz, 2H); 3.88 (dd, *J* = 16.5, 11.0 Hz, 1H); 3.47 (dd, *J* = 16.6, 8.4 Hz, 1H); 2.81 (t, *J* = 6.3 Hz, 2H); 2.35 (s, 3H); 2.11 – 1.98 (m, 2H); 1.89 – 1.73 (m, 2H); 1.47 (q, *J* = 7.4 Hz, 2H); 1.41 – 1.31 (m, 4H); 0.97 – 0.84 (m, 3H). ¹³C NMR (100 MHz, CDCl₃) δ 160.9; 159.7; 158.2; 156.3; 138.1; 137.8; 130.3; 129.7; 129.4; 128.8; 127.4; 126.7; 125.9; 120.5; 119.4; 114.3; 111.6; 82.1; 68.2; 67.3; 43.1; 31.6; 29.7; 29.2; 25.7; 23.9; 22.6; 21.7; 21.2; 14.1. ESI HRMS *m/z* calcd for [M + H]⁺ C₃₄H₃₆N₂O₃ 521.2804; found [M + H]⁺ 521.2811.

7.3.3 5-(4-(*n*-Decyloxy)phenyl)-9-(5-(*p*-tolyl)-4,5-dihydroisoxazol-3-yl)-3,4-dihydro-2H-pyrano[3,2-*c*]quinoline (**7b**). Pale brown solid; yield: 87%; Tg 38°C; ¹H NMR (CDCl₃, 400 MHz) δ = 8.28 – 8.15 (m, 2H); 8.04 (d, *J* = 8.7 Hz, 1H); 7.67 – 7.54 (m, 2H); 7.34 (d, *J* = 8.1 Hz, 2H); 7.21 (d, *J* = 7.9 Hz, 2H); 7.07 – 6.92 (m, 2H); 5.78 (dd, *J* = 10.9, 8.3 Hz, 1H); 4.55 – 4.42 (m, 2H); 4.04 (t, *J* = 6.6 Hz, 2H); 3.91 (dd, *J* = 16.5, 10.9 Hz, 1H); 3.50 (dd, *J* = 16.6, 8.3 Hz, 1H); 2.84 (t, *J* = 6.3 Hz, 2H); 2.38 (s, 3H); 2.06 (td, *J* = 6.3, 4.5 Hz, 2H); 1.84 (q, *J* = 6.3 Hz, 2H); 1.60 – 1.46 (m, 2H); 1.43 – 1.24 (m, 12H); 0.98 – 0.87 (m, 3H). ¹³C NMR (100 MHz, CDCl₃) δ 161.4; 159.5; 157.6; 156.3; 147.9; 138.0; 137.9; 132.3; 130.2; 129.5; 129.4; 126.9; 126.4; 125.9; 120.5; 119.4; 114.3; 111.5; 82.8; 68.2; 67.1; 43.1; 31.9; 29.6; 29.6; 29.4; 29.3; 29.3; 26.1; 24.1; 22.7; 21.9; 21.2; 14.1. ESI HRMS *m/z* calcd for C₃₈H₄₄N₂O₃ [M + H]⁺ 576.3352; found [M + H]⁺ 577.3439.

7.3.4 9-(5-(4-((2-Etylhexyl)oxy)phenyl)isoxazol-3-yl)-5-(4-(*n*-hexyloxy)phenyl)-3,4-dihydro-2*H*-pyrano[3,2-*c*]quinoline (**8**). Pale red solid; yield: 94%; Tg 103 °C; m.p. 122 °C; ¹H NMR (CDCl₃, 400 MHz): δ 8.57 (d, 1H, *J* = 1.5 Hz); 8.21 (dd, 1H, *J* = 8.8 Hz, 1.7 Hz); 8.12 (d, 1H, *J* = 8.8 Hz); 7.81 (d, 2H, *J* = 8.7 Hz); 7.57 (d, 2H, *J* = 8.6 Hz); 7.02 (m, 4H); 6.88 (s, 1H); 4.52 (m, 2H); 4.04 (t, 2H, *J* = 6.6 Hz); 3.93 (d, 2H, *J* = 5.8 Hz); 2.84 (t, 2H, *J* = 6.2 Hz); 2.08 (m, 2H); 1.81 (m, 3H); 1.51 (m, 6H); 1.38 (m, 8H); 0.96 (m, 9H). ¹³C NMR (100 MHz, CDCl₃) δ 170.6; 162.8; 161.3; 161.0; 159.5; 157.8; 147.7; 132.3; 130.2; 129.5; 127.4; 127.4; 126.1; 120.1; 120.0; 119.7; 114.9; 114.3; 111.4; 96.2; 70.7; 68.2; 67.2; 39.3; 31.6; 30.5; 29.2; 29.1; 25.7; 24.1; 23.8; 23.1; 22.6; 21.9; 14.1; 14.0; 11.1. ESI HRMS *m/z* calcd for C₄₁H₅₂N₂O₄ [M + H]⁺ 632.3614; found [M + H] 633.3691.

Author Contributions.

Conceptualization: A. A. M. and L. F.; Data curation: A. A. M., L. F.; L. A. B.; and S. M. S. Formal Analysis: L. F.; L. A. B.; S. M. S and R. J. M.; Funding acquisition: A. A. M.; Investigation and methodology: L. F.; A. A. M., L. A. B.; S. M. S. and R. J. M.; Project administration: A. A. M. and L. F.; Supervision: A. A. M.; S. M. S.; and R. M.; Software: L. A. D. and R. J. M.; Validation: A. A. M. and L. A. B.; Visualization: A. A. M. and L. F.; writing-original draft preparation, A. A. M.; Writing – review & editing: A. A. M. and R. J. M. All authors have read and agreed to the published version of the manuscript.

Declaration of Competing Interest.

The authors declare no competing financial interest.

Data Availability Statement (DAS).

The Data supporting this article have been included at part of the Supplementary Information.

Acknowledgments.

The authors knowledge CNPq/Pq-2023 311195/2023-7 and Fapergs/Edital 07/2021 n. 21/2551-0002121-7, 07/2022 n. 23/2551-0000114-4 for the financial support. L. F. thanks CAPES finance code #001. A. A. M. thanks Ed. 06/2021 RITES – Fapergs and Laboratório Multiusuário de Análise Térmica (LAMAT, IQ, UFRGS).

References

- [1] A.A. Sara, U.-e.-F. Um-e-Farwa, A. Saeed, M. Kalesse, *Synthesis* 54 (2021) 975–998.
- [2] S. Rashid, W.I. Lone, A. Rashid, B.A. Bhat, *Tetrahedron Chem.* 9 (2024) 100066.
- [3] B.L. Oliveira, Z. Guo, G.J.L. Bernardes, *Chemical Society Reviews* 46 (2017) 4895–4950.
- [4] A.A. Merlo, *Reações Pericíclicas. Uma Sinfonia de Moléculas e Elétrons*; Editora da UFRGS: Porto Alegre, RS, Brazil, (2012); p 528.
- [5] V. Eschenbrenner-Lux, K. Kumar, H. Waldmann, *Ang. Chem. Int. Ed.* 53 (2014) 11146–11157.
- [6] L.S. Povarov, *Russian Chem. Rev.* 36 (1967) 656.
- [7] C.D. Smith, J.I. Gavrilyuk, A.J. Lough, R.A. Batey, *J. Org. Chem.* 75 (2010) 702–715.
- [8] V.V. Kouznetsov, C.M. Meléndez Gómez, M.G. Derita, L. Svetaz, E. del Olmo, S.A. Zacchino, *Bioorg. Med. Chem.* 20 (2012) 6506–6512.
- [9] N. Atanes, L. Castedo, E. Guitian, C. Saa, J.M. Saa, R. Suau, *J. Org. Chem.* 56 (1991) 2984–2988.
- [10] R.R. Singh, T.P. Singh, N.P. Singh, S.S. Naorem, O.M. Singh, *J. Fluoresc.* 31 (2021) 247–257.
- [11] G.C. dos Santos, R.O. Servilha, E.F. de Oliveira, F.C. Lavarda, V.F. Ximenes, L.C. da Silva-Filho, *J. Fluoresc.* 27 (2017) 1709–1720.
- [12] E. Sales, J. Schneider, M. Santos, A. Bortoluzzi, D. Cardoso, W. Santos, A. Merlo, *J. Braz. Chem. Soc.* 26 (2015) 562–571.
- [13] G. Lewinska, J. Sanetra, K.W. Marszalek, *J. Mater. Sci.: Mater. Electron.* 32 (2021) 18451–18465.
- [14] A. Santoro, A.C. Whitwood, J.A.G. Williams, V.N. Kozhevnikov, D.W. Bruce, *Chem. Mater.* 21 (2009) 3871–3882.
- [15] U.B. Vasconcelos, A.A. Merlo, *Synthesis* (2006) 1141–1147.
- [16] U.B. Vasconcelos, E. Dalmolin, A.A. Merlo, *Org. Lett.* 7 (2005) 1027–1030.
- [17] K. Schiemann, D. Finsinger, F. Zenke, C. Amendt, T. Knöchel, D. Bruge, H.-P. Buchstaller, U. Emde, W. Stähle, S. Anzali, *Bioorg. Med. Chem. Lett.* 20 (2010) 1491–1495.
- [18] Y. Makioka, T. Shindo, Y. Taniguchi, K. Takaki, Y. Fujiwara, *Synthesis* 7 (1995) 801–804.
- [19] R. Suresh, S. Muthusubramanian, R. Senthilkumaran, G. Manickam, *J. Org. Chem.* 77 (2012), 1468–1476.
- [20] A. Merlo, H. Gallardo, T.R. Taylor, T. Kroin, *Mol. Cryst. Liq. Cryst. Sci. Technol. Sect. Cryst. Liq. Cryst.* 250 (1994) 31–39.
- [21] L. Fritsch, L.A. Baptista, I.H. Bechtold, G. Araújo, R.J. Mandle, A.A. Merlo, *J. Mol. Liq.* 298 (2020) 111750.
- [22] J. Cabral, P. Laszlo, *Tetrahedron Lett.* 30 (1989) 7237–7238.
- [23] L. Fritsch, A.A. Merlo, *ChemistrySelect* 1 (2016) 23–30.
- [24] L. Fritsch, V. Lavayen, A.A. Merlo, *Liq. Cryst.* 45 (2018) 1802–1812.
- [25] J.-M. Lehn, *Chem. - Eur. J.* 12 (2006) 5910–5915.
- [26] A. Iwan, H. Janeczek, B. Jarzabek, P. Rannou, *Materials* 2 (2009) 38–61.
- [27] K. Geibel, B. Staudinger, K.H. Grellmann, H. Wendt, *J. Photochem.* 3 (1974) 241–246.
- [28] C. Cimorelli, S. Bordi, P. Piermattei, M. Pellei, F. Del Bello, E. Marcantoni, *Synthesis* 49 (2017) 387–95.
- [29] J. Clerigué, M.T. Ramos, J.C. Menéndez, *Org. & Biomol. Chem.* 20 (2022) 1550–81.
- [30] R. M. Limantseva, R. G. Savchenko, V. N. Odínokov, A.G. Tolstikov, *Russian J. Org. Chem.* 59 (2023) 1102–1135.
- [31] C. Masdeu, J.M. de los Santos, F. Palacios, C. Alonso, *Top. Curr. Chem.* 381 (2023) 1–20.

- [32] Y.A. Rodríguez-Núñez, J. Sánchez-Márquez, J. Quintero-Saumeth, C.J. Guerra, E. Polo-Cuadrado, D. Villaman, C.A. Fica-Cornejo, A.R.R. Bohórquez, *RSC Advances* 15 (2025) 11799-810.
- [33] L.R. Domingo, M.J. Aurell, J.A. Sáez, S.M. Mekelleche, *RSC Advances* 4 (2014) 25268-78.
- [34] V.V. Kouznetsov, *Tetrahedron* 65 (2009) 2721–2750.
- [35] V.W. Bowry, K.U. Ingold, *J. Am. Chem. Soc.* 114 (1992) 4992–4996.
- [36] R. Leardini, D. Nanni, A. Tundo, G. Zanardi, G.F. Pedulli, *Liq. Cryst.* 2 (1987), 625–631.
- [37] Y. Zhou, M. Zhang, M. Yin, X. Wang, *Chin. J. Chem.* 31 (2013) 237–242.
- [38] X.-S. Wang, J. Zhou, M.-Y. Yin, K. Yang, S.-J. Tu, *J. Comb. Chem.* 12 (2010) 266–269.
- [39] B. Crousse, J.-P. Bégué, D. Bonnet-Delpon, *J. Org. Chem.* 65 (2000) 5009–5013.
- [40] M.V. Spanedda, V.D. Hoang, B. Crousse, D. Bonnet-Delpon, J.-P. Bégué, *Tetrahedron Lett.* 44 (2003) 217–219.
- [41] L.C. da Silva-Filho, V. Lacerda Júnior, M.G. Constantino, G.V.J. da Silva, *Synthesis* 16, (2008) 2527–2536.
- [42] F. Neese, *Wiley Interdiscip. Rev.: Comput. Mol. Sci.* 2 (2012) 73–78.
- [43] V. Barone, M. Cossi, *J. Phys. Chem. A* 102 (1998) 1995–2001.